Self-healing three-dimensional bulk materials based on core-shell nanofibers

Min Wook Lee[1,2], Seongpil An[3], Yong-Il Kim[3], Sam S. Yoon[3]*, Alexander L. Yarin[1]*

[1]Department of Mechanical and Industrial Engineering, University of Illinois at Chicago, 842 W. Taylor St., Chicago IL 60607-7022, USA

[2]Multifunctional Structural Composite Research Center, Institute of Advanced Composites Materials, Korea Institute of Science and Technology, Chudong-ro 92, Bondong-eup, Wanju-gun, Jeollabuk-do, 55324, Republic of Korea

[3]School of Mechanical Engineering, Korea University, Seoul 136-713, Republic of Korea

KEYWORDS: self-healing, core-shell fibers, three-dimensional, composite, sponge

ABSTRACT

In this study, electrospun core-shell nanofibers containing healing agents are embedded into a three-dimensional bulk matrix in a simple versatile process. Two types of the healing agents (resin monomer and cure) are encapsulated inside the nanofiber cores. The core-shell fibers are

Formatted: Not Highlight

encased in the macroscopic three-dimensional bulky material. To achieve this goal, the electrospun core-shell fibers containing two components of PDMS (either resin monomer or cure) are directly embedded into an uncured PDMS bath and dispersed there, essentially forming a monolithic composite. For the evaluation of the self-healing features, the interfacial cohesion energy is measured at the cut surface of such a material. Namely, the bulk of the prepared self-healing material is entirely cut into two parts using a razor blade and then re-adhered due to the self-curing process associated with the released healing agents. The results reveal that the self-healing fiber network works and releases a sufficient amount of resin monomer and cure at the cut surface to facilitate self-healing. In addition, chopped into short filaments core-shell fibers were embedded into highly porous sponge-like media. After a mechanical damage in compression or shearing fatigue, this sponge-like material also revealed restoration of stiffness due to the released self-healing. The sponges revealed a 100% recovery and even enhancement after being damage in the cyclic compression and shearing tests, even though only 0.086% of the healing agents were embedded per sponge mass and finely dispersed in it.

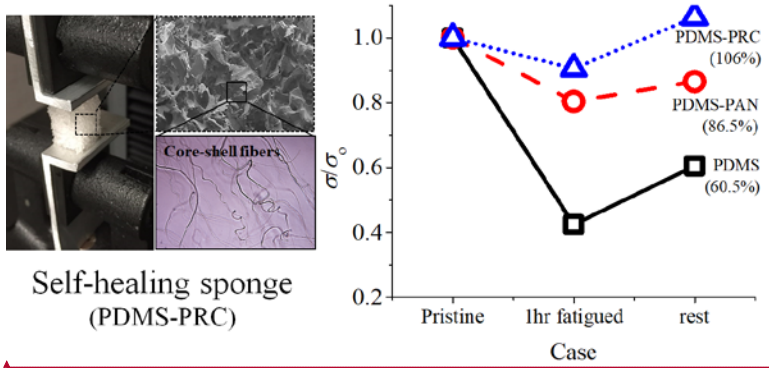

Corresponding authors: A.L. Yarin (ayarin@uic.edu), S.S. Yoon (skyoon@korea.ac.kr)

Formatted: Not Highlight

Formatted: Not Highlight

Formatted: Not Highlight

Formatted: Not Highlight

Formatted: Not Highlight

1. Introduction

Self-healing is one of the fascinating and desirable features of engineered materials that has been sought to be adopted from nature. For the last two decades, the research area related with this topic emerged which deals with development of new healing materials and methods [1-13]. At the early stage, microcapsules and hollow fibers were used. They were viable albeit bulky, which can not only heal but also inherently weaken the structural stability [2, 4, 14, 15]. That is why scaling-down of the healing elements was aimed at, potentially to the microscopic and nano-sizes. Nanofibers encapsulating healing agents were remarkably beneficial for the effective self-healing [16-18], in comparison with the capsule-type self-healing. Indeed, nanofibers are inter-connected and form a network, which is capable of supplying healing agents toward a damaged and depleted area, and thus facilitate healing [7, 19, 20]. Given weight restrictions related to the base composite material, it is typically preferable to employ thin nanofibers rather than capsules on a few-micrometer scale. Similarly, electrospun nanofibers were utilized to replace micro-scaled tubing [17, 21]. A self-healing thin nanofiber layer demonstrated successful healing and restoration of mechanical properties following tensile, bending and delamination damages [10, 18, 22-25]. A relatively inexpensive and straightforward fabrication method of electrospinning [26] is one of the attractive techniques for development of self-healing materials.

However, this was essentially done for only thin samples and inter-layers, and it is still challenging to develop a macroscopic bulky three-dimensional self-healing material based on nanofibers. This would involve an effective self-healing spanning the microscopic to macroscopic level. In doing so, the problem of a continuous supply of self-healing agents embedded in a bulky material on nano-scale and spanning it up to macroscopic level can be solved. This is aimed at in

the present study, where bulky 3D materials are prepared with embedded self-healing core-shell nanofibers. Thick blocks of such self-healing materials are expected to reattach and heal after being cut in half. Another type of a 3D sponge-like material with self-healing properties is also in focus in the present work.

Bulky self-healable materials are of interest in multiple engineering, for example, bio-mimetic and biomedical applications. Sponge-like materials are beneficial due to their low density and softness. They are tremendously effective as liquid absorber [27], compression-shock dampers, cleaners, etc. Their intrinsic porosity facilitates embedding of self-healing nanofibers, and their self-healing properties would mimic multiple natural materials derived from humans, animals, and plants.

2. Experimental

2.1. Materials and sample preparation

2.1.1. Three-dimensional block

PDMS (polydimethylsiloxane, Sylgard 184) was purchased from Dow Corning, PAN (polyacrylonitrile , M_w = 150 kDa) and DMF (dimethylformamide, 99.8%) were purchased from Sigma Aldrich. The two components of PDMS, resin (dimethyl siloxane) and cure (dimethyl-methyl hydrogen-siloxane), were embedded separately within the cores of the individual PAN fibers by coaxial electrospinning [26]. The overall co-electrospinning conditions were similar to those used in our works before [22, 23], except for the substrate. Two parts of PDMS, resin monomer and cure, were supplied into core-shell PAN fibers using co-electrospinning technique.

The co-electrospun core-shell fibers had either resin monomer or cure in the core and PAN in the shell. The resin monomer and cure stored in the fiber cores stay liquid unless they come in contact to each other after the material has been damaged.

It should be emphasized that a specific polymer is chosen according to the required spinnability in different spinning system. In our previous works [13, 26] PVDF/PEO blends in acetone/DMF were used in the solution blowing process, whereas in the present study PAN in DMF is used in co-electrospinning. Spinnability of a particular polymer solution typically depends on its viscoelasticity (associated primarily with the polymer molecular weight and concentration in solution) and spinning conditions [26]. The spinning conditions determine the driving forces of the process, and in particular, the rates of stretching involved. Some polymer solutions which work properly in electrospinning, do not necessarily work properly in solution blowing and vice versa. In the present case, however, both PVDF/PEO or PAN could be used. PAN in DMF is a relatively easily co-electrospinnable, and thus attractive solution to be used.

The premixed (10:1 ratio) PDMS (V = 55 ml), which was not cured yet, was placed in the petri dish located under the co-electrospinning nozzles as shown in Figure 1. Then, the fibers containing two separate components of PDMS (either the resin monomer, or cure) were simultaneously co-electrospun onto an uncured liquid PDMS (pre-mixed resin and cure which was not polymerized yet) located in the petri dish for 30 min to 2 h with the fixed core and shell flow rates of 90 μL/h and 550 μL/h, respectively. The bottom of the PDMS bath was a steel substrate which was grounded. The voltage applied to both co-electrospinning syringes was 11.5 kV, and the distance between the nozzle and the uncured PDMS was 8 cm. The co-electrospun fibers, which touched the surface of liquid PDMS were wet and submerged in it. After that, the sample in the petri dish was dried for 48 h up to solidification at room temperature. To prepare a three-

layered 3D block of self-healing material, the uncured PDMS was firstly prepared as a single layer. Then, the first co-electrospinning was conducted for 30 min, as described above. To form the second layer onto the first layer, the nanofiber-embedded uncured PDMS was half-dried for 24 h and the second co-electrospinning was then conducted for 30 min. Similarly, the third layer was prepared by the same process as the second layer. Note that the second drying time was 24 h and the third drying time was 48 h.

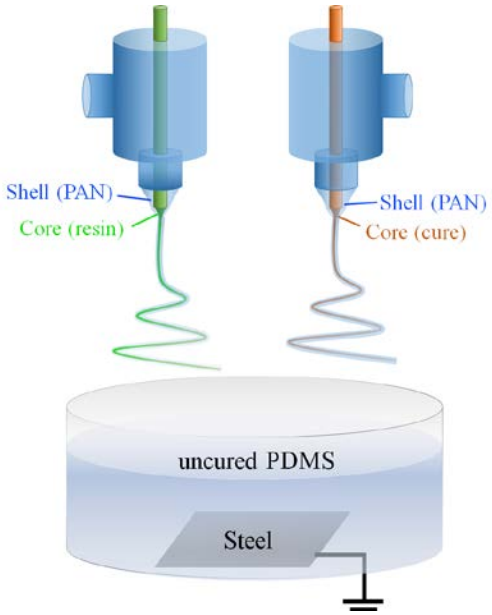

Figure 1. Schematic of dual coaxial-electrospun core-shell fiber submerged into uncured PDMS in petri dish with grounded bottom.

2.1.2. Sponge

The sugar frame of a sponge was prepared with sugar grains (organic turbinado raw cane sugar) purchased at local grocery. The core-shell fibers with self-healing agents were electrospun from the coaxial nozzle. 8 wt% of PAN was dissolved in DMF to form shell material. For the core, one of the two parts of PDMS, resin monomer was diluted with hexane in the 2:1 wt% ratio, while the other part, the curing agent, was used as it is. It should be emphasized that healing agents are selected according to the application circumstances. Under some conditions, the curing time needs to be shortened, so that the healing process proceeds in faster, and the mechanical stiffness and strength are recovered faster. In the present work, PDMS is sufficient to reveal characteristics of these novel three-dimensional materials, even though its solidification time is longer and strength is lower than those of epoxy [13].

The fiber mat was deposited onto a rotating drum collector for 3 h. The details of the preparation of self-healing fiber mat are the same as those described above for the 3D block preparation.

A porous three-dimensional PDMS sponge is prepared as shown in Figure 2. The 0.2 g of the as-spun fiber mat (PAN or PRC, the latter stands for polymer-resin-cure, i.e. the core-shell fibers with one of the healing agents in the core) was chopped using a commercial food chopper (Ninja NJ100GR) for 4 min within 50 ml of resin. A part of the healing agent can be released from the edges of the chopped fibers, similarly to the observations of the release process in a larger scale in [28]. However, a partial recovery of the mechanical properties after damage discussed below in relation to Figure 8, shows that there is still enough healing agents left in the cores of the chopped core-shell nanofibers embedded in a sponge. The chopped fibers were roughly of a length of 20-50 μm (see Figure 7b below). Then, 5 ml of the curing agent were add to that colloidal solution and mixed well (PDMS with chopped fibers premixed in the ratio of 10:1 to the cure). After that,

the fiber-PDMS mixed solution was poured onto the sugar skeleton and then left in a vacuum chamber for 24 h for the curing process to proceed. Then, the PDMS-infiltrated sugar frame was rinsed in a hot water bath and sonicated for 10 min, which facilitated removal of the sugar in the cube. The PDMS-PAN (or PRC) sponge shaped by sugar skeleton, but without sugar, was then dried in an oven for 30 min at 100 °C. The mass ratio of the embedded fibers to the PDMS matrix in the sponge is found as 0.2 g / (55 ml × 0.965 g/ml) × 100% =3.77%, and the core-to-shell mass ratio in the embedded coelectrospun fibers was 2.29% as in [13].

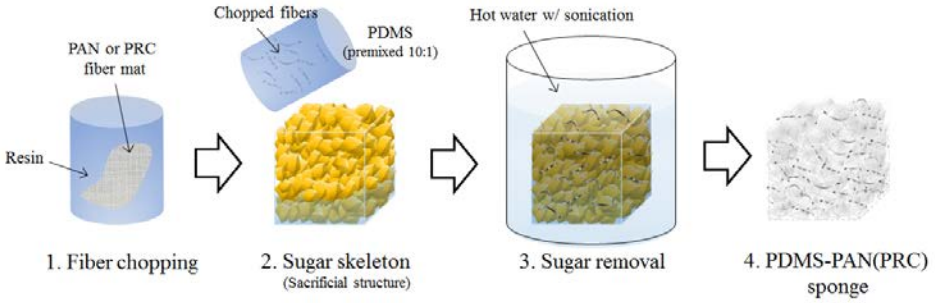

Figure 2. Fabrication of self-healing sponge.

2.2 Self-healing evaluation

2.2.1 Adhesion test (for the 3D block)

The prepared 3D PDMS block samples with sizes 15×7×20 mm^3 (w×d×l, see Figure 3d) were completely cut into two parts by a razor blade and then re-attached manually. Then, the samples were left for 2 days under atmospheric conditions without any further treatment. In 2 days, the samples are tested in tensile tests with stretching normal to the cut to determine the interfacial adhesion energy, which emerged due to self-healing during the 2 days (Figure 3). Two pins

(*d*=3.15 mm) were placed through the punched holes in the middle of the upper/lower body of a sample. Each pin was attached to a plate, which was held by the upper/lower grip of the Instron 5942 system with a 100 N load cell. As the tensile machine (Instron 5942) stretched the sample, the force required to disconnect the self-healed scar in the sample was recorded with the corresponding extension. This force, essentially, the adhesion force, was measured for all the samples with and without (w/ and w/o) self-healing core-shell fibers embedded inside. If the self-healing fibers would 'work' properly at the cut interface (i.e. would release the resin monomer and cure stored in the core in a sufficient amount), a non-zero adhesion force (and thus adhesion energy) would be measured in this test.

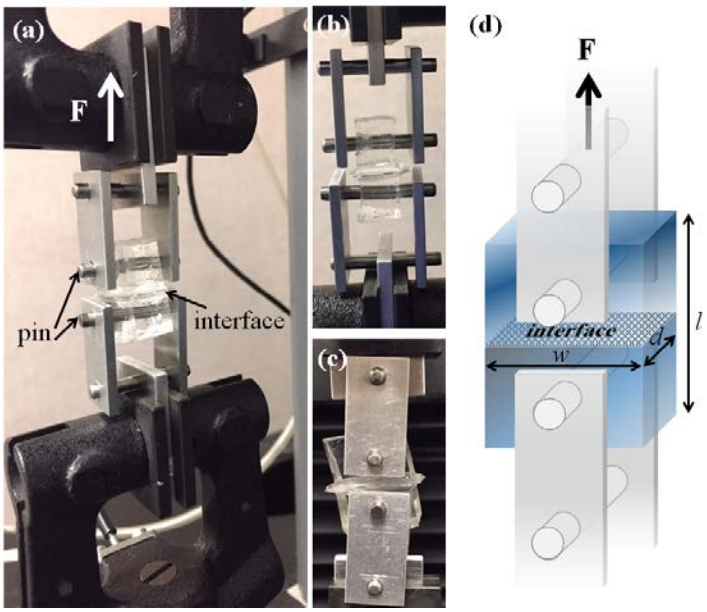

Figure 3. (a) Setup used to measure interfacial adhesion at the self-cured surface. (b) Side view (c) Front view. (d) Schematic.

2.2.2 Compression test (for self-healing sponge)

Three different types of sponges, pure PDMS, PDMS-PAN and PDMS-PRC, were cut in samples with dimensions of 10×10×15 mm^3 (w×w×h) and then subjected to the compression test for the self-healing characterization (see Figure 4). The strain-stress curves in the compressive tests were obtained with the up to 60% of compression at a compression rate of 10 mm/min using Instron 5942 (Figure 4a). For the fatigue tests, similar samples were cyclically compressed for 3600 times up to ε=60% compression at frequency of f=1 Hz (Figure 4b).

Formatted: Not Highlight

Formatted: Not Highlight

2.2.3 Shearing fatigue test (for self-healing sponge)

Formatted: Not Highlight

In addition to the cyclic compression of sub-section 2.2.2, the cyclic shear fatigue test of the PDMS-PRC sponge was conducted for 3600 times at frequency of f =1 Hz using a modified version of the setup shown in Figure 4b.

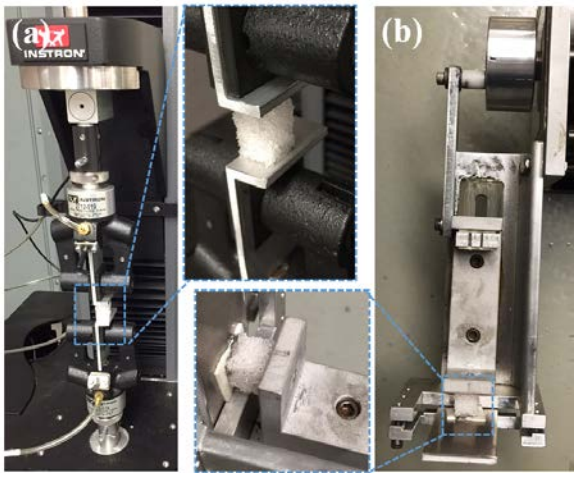

Figure 4. (a) Setup for compression test. (b) Cyclic compression setup. A modified version of this setup realized cyclic shearing test.

Formatted: Not Highlight

2.3. Characterization

The SEM (Scanning Electron Microscope) and optical microscope images were obtained by Hitachi S-3000N at 5 kV and Olympus BX-51. An inner SEM image of the 3D block sample was obtained by using a dual beam focused ion beam (FIB, LVRA3 XMH, TESCAN) and field-emission scanning electron microscope (FE-SEM, Quanta 250 FEG, FEI). The non-destructive 3D image was obtained by micro-CT (SkyScan 1172, Bruker) at 72 kV.

Formatted: Not Highlight

3. Results and Discussion

3.1. 3D block

To observe the inner structure of the 3D block with the embedded fibers, a cross-sectional SEM image of the 3D block was obtained by focused ion beam (FIB) milling, as shown in Figure 5a. Even though it seems that the ends of the embedded fibers were damaged (or melted) due to the high thermal energy involved in the FIB process, the traces of the embedded fibers were clearly visible. The reinforcing fibers embedded in the composite material were observed in the literature along the fractured surface [29]. If a matrix material is brittle, the individual fibers can be seen at the fractured surface. However, at a clean cut surface of the elastic matrix material as in the present study, only dots corresponding to the fibers are seen in the SEM image (cf. Figure 5a). On the

Formatted: Not Highlight

Formatted: Not Highlight

other hand, the embedded fibers and epoxy drops released due to mechanical damage were found to be clearly seen in the optical microscope images (Figures 5b and 5c).

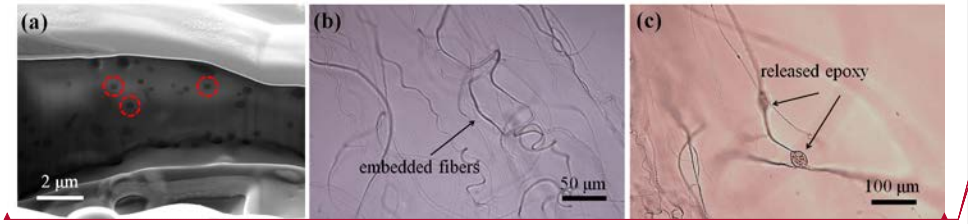

Figure 5. (a) The inner SEM image of the FIB-treated 3D block sample. Several cut edges of the embedded fibers with self-healing materials are encircled by dashed red circles. TEM images of the embedded nanofibers, which reveal their core-shell structure in full detail are available in our previous works [22,23]. Magnification: ×22600. (b) The optical microscope image of the undamaged embedded fibers. (c) The optical microscope images of the released epoxy in a 3D block sample after mechanical damage. Magnification: ×10.

The tensile tests for samples of each kind were repeated thrice to evaluate repeatability, of which one was sample was too weak to allow measurement. So the results reported below were obtained for two samples. The measured entire load-extension curves and the peak points (the ultimate force and extension-at-failure), as well as the evaluated values of the adhesion for each curve are shown in Figures 6 a and b, respectively. Figure 6b reveals that the adhesion energy of the samples containing fibers increased as the deposition time increased from 0.5 to 2 h. A higher adhesion energy is associated with a larger number of fibers embedded in the composite, since more fibers are capable of releasing more healing agents and thus achieving a higher interfacial adhesion energy (cf. Figure 6b). It is noteworthy that the case with three layers of the embedded

Formatted: Not Highlight

Formatted: Not Highlight

Formatted: Not Highlight

self-healing fibers revealed the highest adhesion energy. It means that not only the number of the embedded fibers but also the distribution of fibers in the bulk is important for the efficient healing. In comparison with the ordinary samples with 2 h of fiber deposition, the three-layer sample may even have less fibers (due to a shorter deposition time of 1.5 h), albeit be more effective from the self-healing point of view due to a better fiber distribution.

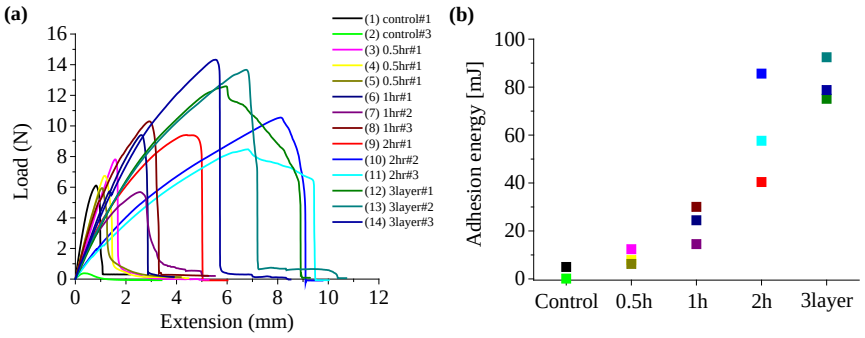

Figure 6. (a) Load-extension curve. (b) Adhesion energy. In both panels the following data is presented. Control: a composite sample embedded with the ordinary fibers (not self-healing fibers); a composite sample embedded with self-healing fibers deposited for 0.5/1/2 h; a three-layer composite sample embedded with self-healing fibers with three separated times of deposition. Each layer was deposited for 0.5 h upon a partially-cured PDMS bath after 6 h of curing time. In panel (a) -#: is the case number. In panels (a) and (b) the identical colors correspond to the same set of data.

3.2. Sponge

The as-prepared sponges were observed using SEM and optical microscope. The irregular and non-uniform structure of the PDMS sponge is seen in Figure 7a-d. The tails of PAN and PRC fibers embedded in the PDMS matrix are seen at the cut surface of sponge in the magnified second images in Figures 7c and 7d. The sponge porosity is calculated accounting for the amount of 30 ml PDMS in the sugar skeleton of 56.4 ml, as (1–30/56.4)×100% = 46.81%. The pore size is approximated by the grain size of sugar granules, which ranges from 0.6 to 1.5 mm. It should be emphasized that when the core-shell fibers are observed in micro-scale, it is quite easy to find the epoxy released from the cut fibers (such image is available in our previous work [13]). It is much more difficult to observe the epoxy release from thin nanofibers because they easily melt or burnt under a focused SEM beam, and thus a higher-magnification image of release from a damaged individual fiber is typically impossible to obtain (albeit, see Figure 6 in our previous work [21]). In the present work we chose tests, which revealed repairing of mechanical damage, to demonstrate the effect of the released healing agents and a successful healing process. The micro-CT, the non-destructive imaging method was also used to observe the porous structures of the sponge. However, this method was incapable of also visualizing the embedded fibers in the matrix material, since the fiber cross-sectional diameter is smaller than the minimum resolution (~1 μm) of the micro-CT equipment (see Figure 7e).

Formatted: Not Highlight

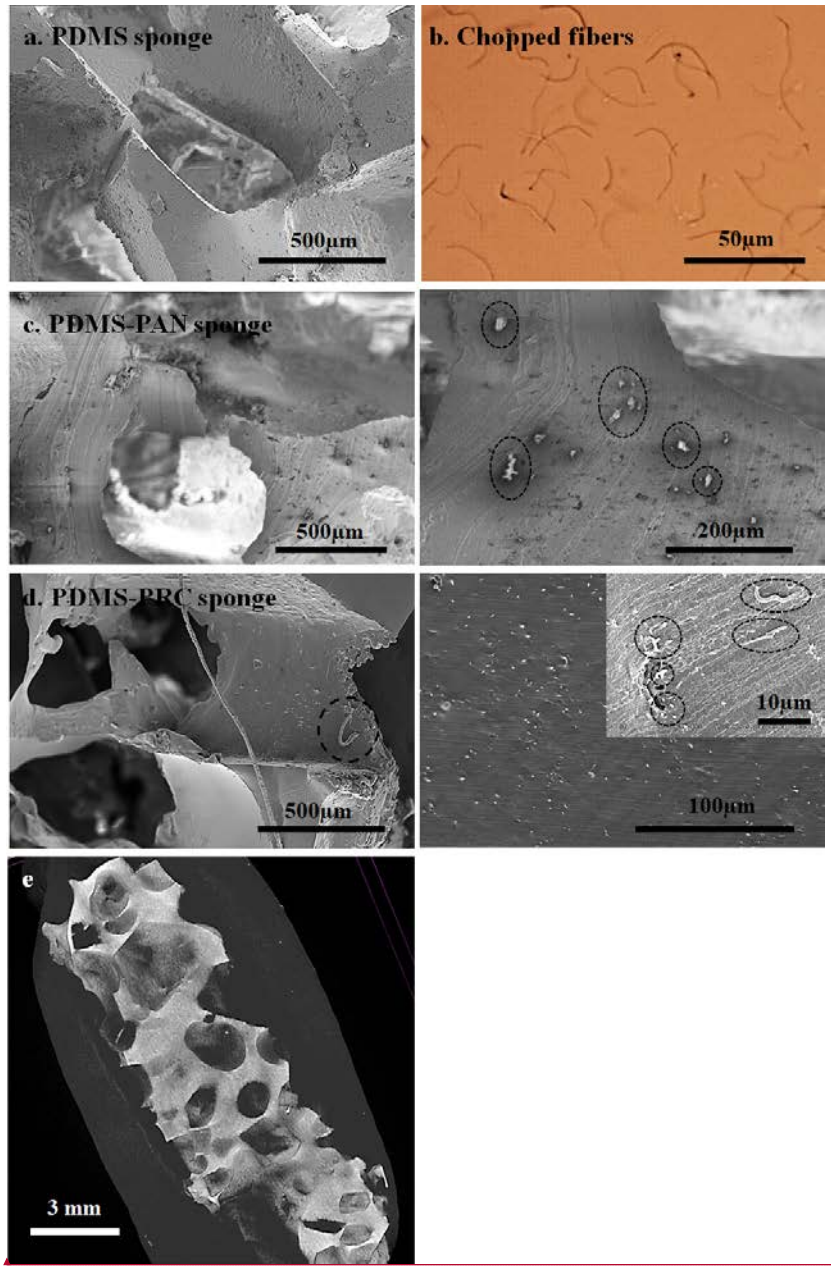

Formatted: Not Highlight

Figure 7. (a) PDMS sponge. (b) Chopped fibers. (c) PDMS-PAN sponge. (d) PDMS-PRC sponge. In panels (c) and (d) in the enlarged images on the right, several cut or aligned nanofibers are encircled by dashed curves. Magnification: ×80, ×800, ×70/×200, ×80/×500 for panels a-d, respectively. (e) The micro-CT image of PDMS-PRC sponge.

Formatted: Not Highlight

The pure PDMS sponge and PAN/PRC fiber-reinforced PDMS sponges were compressed until the strain of 60 %. The corresponding stress-compression curves are shown in Figure 8a. It is seen that the presence of PAN and PRC fiber embedded in the PDMS matrix weakens the composite. The stress-strain curve in compression were measured using (a) a pristine (without any loading at first) sample, (b) and an identical sample right after the repeated compression in the fatigue test for 1 h, or (c) using the samples left for 2 days after the fatigue test. As shown in Figure 8b, the rubber-like pure PDMS matrix material partially restored its mechanical properties after a certain level of damage in compressive fatigue test without any interference of self-healing nanofibers [cf. σ/σ_o = 42.4% at the compression strain ε=60.5% in Figure 8e, where σ is the compressive stress revealed by the damaged and 'restored' material, while σ_o is the stress revealed by the undamaged sample]. The PDMS-PAN sponge also partially restored its mechanical properties [(σ/σ_o) increased from 80.4 to 86.5% at the strain ε=60.5%; cf. Figure 8e]. On the other hand, the PDMS-PRC sponge containing self-healing nanofibers revealed the highest restoration of the mechanical properties [(σ/σ_o) increased from 90.5 to 106.4% at the strain ε=60.5%], even to the level higher than the original one, as is seen in Figure 8e.

The mechanical behavior of samples in compression was also tested after they underwent the preceding cyclic shearing fatigue. As shown in Figure 8f, the PDMS-PRC sponge sample also revealed the robust highest restoration of the mechanical properties compression, even though they were damaged in the preceding cyclic shearing fatigue test. Namely, the ratio σ/σ_0 increased from 96.8 to 105.5% at the strain ε = 60.5%.

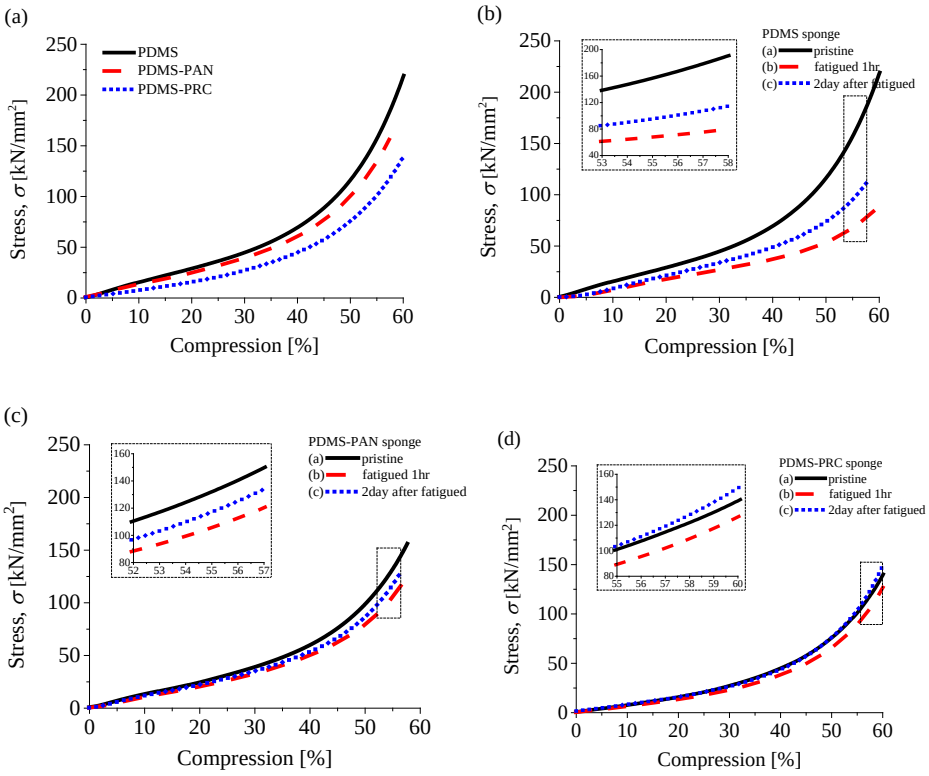

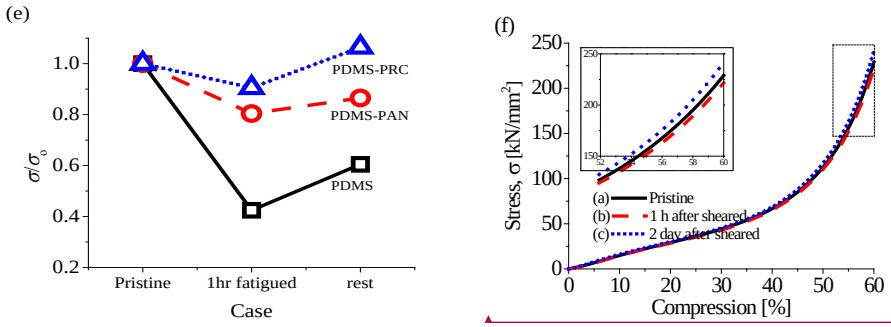

Figure 8. Compression test. (a) Pristine sponges. (b) Pure PDMS sponge (10.87×10.63×16.18 mm^3) (c) PDMS-PAN sponge (10.11×10.27×16.57 mm^3) without self-healing materials. (d) PDMS-PRC sponge (10.06×9.60×15.08 mm^3), with self-healing materials (e) Compressive stress (σ) measured in damaged material vs. the compressive initial stress (σ_0) in the same material, at the compressive strain ε=60%. (f) Stress-strain curves in compression of samples which underwent preceding shearing fatigue in comparison with the pristine sample.

In the other three-dimensional self-healing bulky materials described in the literature [30, 31], the vascular structures containing healing agents were made of hollow tubing or sacrificial fibers (e.g. glass fibers), fugitive inks, etc. The healing efficiency in those studies was reported to be about 70-80% judging by the mechanical property recovery in tensile or bending tests. In comparison, Figure 8e reveals an approximately 85-100% recovery observed in the present work for the self-healing sponge in compression test after cyclic compression fatigue test and Figure 8f demonstrates practically 100% recovery after cyclic shearing text.

Formatted: Not Highlight

Formatted: Not Highlight

Formatted: Not Highlight

4. Conclusion

Three-dimensional self-healing materials were formed as the 3D PDMS blocks with the embedded co-electrospun core-shell nanofibers with the self-healing agents (resin monomer or cure) being encapsulated separately in the cores. These 3D blocks were cut and then re-attached. As a result of curing due to the released materials at the newly formed interface (instead of the cut), it was self-healed and the associated adhesion energy was measured in the tensile test.

Another type of three-dimensional self-healing material was formed using a porous 3D sugar skeleton impregnated either with pure PDMS, or PDMS with the embedded chopped self-healing co-electrospun core-shell fibers. After that, the sacrificial sugar skeleton was removed and sponges (non-self-healing and self-healing) were obtained. These sponges were damaged by compression or in periodic compressive or shearing fatigue tests. Then, their mechanical properties were studied. It was found the self-healing sponges revealed an amazing full recovery of their original mechanical properties, and more than that, even an additional stiffening. It should be emphasized that this was achieved with only 0.086% of the healing agents per sponge mass, albeit finely dispersed over the entire sponge skeleton. Therefore, the tips of micro-cracks resulting from fatigue damage had a high probability of intersecting a self-healing fiber. Accordingly, healing agents were released and healed the cracks. Micro-cracks definitely did not constitute more than 0.086% of the sponge wall volume, and stitching the crack banks, as shown in [28], would require even less healing agent than the available 0.086%.

Formatted: Not Highlight

Formatted: Not Highlight

In the previous studies in the literature where self-healing three-dimensional bulky materials were developed, most of the vascular structures were made of hollow tubing or sacrificial fibers such as glass fibers, fugitive inks, etc., or a narrow layer of nanofibers. So the truly three-

dimensionally dispersed self-healing nanofibers in a three-dimensional bulky material were demonstrated for the first time in the present work, as to our knowledge.

Acknowledgement

This work was supported by the International Collaboration Program funded by the Agency for Defense Development of the Republic of Korea.

References

[1] M.R. Kessler, S.R. White, Self-activated healing of delamination damage in woven composites, Composites: Part A 32 (2001) 683-699.
[2] E.N. Brown, N.R. Sottos, S.R. White, Fracture testing of a self-healing polymer composite, ExM 42 (2002) 372-379.
[3] E.N. Brown, S.R. White, N.R. Sottos, Microcapsule induced toughening in a self-healing polymer composite, J. Mater. Sci. 39 (2004) 1703–1710.
[4] S.H. Cho, H.M. Andersson, S.R. White, N.R. Sottos, P.V. Braun, Polydimethylsiloxane-based self-healing materials, Adv. Mater. 18 (2006) 997-1000.
[5] H.R. Williams, R.S. Trask, I.P. Bond, Self-healing composite sandwich structures, SMaS 16 (2007) 1198-1207.
[6] S. Burattini, H.M. Colquhoun, J.D. Fox, D. Friedmann, B.W. Greenland, P.J.F. Harris, W. Hayes, M.E. Mackay, S.J. Rowan, A self-repairing, supramolecular polymer system: Healabilityas a consequence of donor–acceptor π–π stacking interactions, Chem. Commun. (2009) 6717-6719.
[7] C.J. Hansen, W. Wu, K.S. Toohey, N.R. Sottos, S.R. White, J.A. Lewis, Self-healing materials with interpenetrating microvascular networks, Adv. Mater. 21 (2009) 4143-4147.
[8] D. Greig, Self-healing car paint uses sunlight to repair scrapes, The TIMES, 2009.
[9] G.J. Williams, I.P. Bond, R.S. Trask, Compression after impact assessment of self-healing cfrp, Composites A 40 (2009) 1399-1406.
[10] M.W. Lee, S. An, C. Lee, M. Liou, A.L. Yarin, S.S. Yoon, Hybrid self-healing matrix using core−shell nanofibers and capsuleless microdroplets, ACS Appl. Mater. Interfaces 6 (2014) 10461−10468.
[11] A. Das, A. Sallat, F. Bohme, M. Suckow, D. Basu, S. Wießner, K.W. Stockelhuber, B. Voit, G. Heinrich, Ionic modification turns commercial rubber into a self-healing material, ACS Appl. Mater. Interfaces 7 (2015) 20623-20630.
[12] A.R. Jones, C.A. Watkins, S.R. White, N.R. Sottos, Self-healing thermoplastic-toughened epoxy, Polymer 74 (2015) 254-261.
[13] M.W. Lee, S.S. Yoon, A.L. Yarin, Solution-blown core−shell self-healing nano- and microfibers, ACS Appl. Mater. Interfaces 8 (2016) 4955−4962.
[14] E.N. Brown, S.R. White, N.R. Sottos, Microcapsule induced toughening in a self-healing polymer composite, J. Mater. Sci. 39 (2004) 1703-1710.
[15] J.W.C. Pang, I.P. Bond, A hollow fibre reinforced polymer composite encompassing self-healing and enhanced damage visibility, Compos. Sci. Technol. 65 (2005) 1791-1799.
[16] J.-H. Park, P.V. Braun, Coaxial electrospinning of self-healing coatings, Adv. Mater. 22 (2010) 496-499.
[17] X.-F. Wu, A. Rahman, Z. Zhou, D.D. Pelot, S. Sinha-Ray, B. Chen, S. Payne, A.L. Yarin, Electrospinning core-shell nanofibers for interfacial toughening and self-healing of carbon-fiber/epoxy composites, J. Appl. Polym. Sci. 129 (2012) 1383-1393.
[18] M.W. Lee, S. An, C. Lee, M. Liou, A.L. Yarin, S.S. Yoon, Self-healing transparent core-shell nanofiber coatings for anti-corrosive protection, J. Mater. Chem. A 2 (2014) 7045-7053.
[19] S.R. White, N.R. Sottos, P.H. Geubelle, J.S. Moore, M.R. Kessler, S.R. Sriram, E.N. Brown, S. Viswanathan, Autonomic healing of polymer composites, Nature 409 (2001) 794-797.
[20] D.Therriault, R.F. Shepherd, S.R. White, J.A. Lewis, Fugitive inks for direct-write assembly of three dimensional microvascular networks, Advanced Materials 17 (2005) 394–399.
[21] S. Sinha-Ray, D.D. Pelot, Z.P. Zhou, A. Rahman, X.-F. Wub, A.L. Yarin, Encapsulation of self-healing materials by coelectrospinning, emulsion electrospinning, solution blowing and intercalation, J. Mater. Chem. 22 (2012) 9138-9146.

[22] S. An, M. Liou, K.Y. Song, H.S. Jo, M.W. Lee, S.S. Al-Deyab, A.L. Yarin, S.S. Yoon, Highly flexible transparent self-healing composite based on electrospun core-shell nanofibers produced by coaxial electrospinning for anti-corrosion and electrical insulation Nanoscale 7 (2015) 17778-17785.
[23] M.W. Lee, S. An, H.S. Jo, S.S. Yoon, A.L. Yarin, Self-healing nanofiber-reinforced polymer composites: 1. Tensile testing and recovery of mechanical properties, ACS Appl. Mater. Interfaces 7 (2015) 19546-19554.
[24] M.W. Lee, S. An, H.S. Jo, S.S. Yoon, A.L. Yarin, Self-healing nanofiber-reinforced polymer composites: 2. Delamination/debonding, and adhesive and cohesive properties, ACS Appl. Mater. Interfaces 7 (2015) 19555-19561.
[25] M.W. Lee, S. Sett, S.S. Yoon, A.L. Yarin, Fatigue of self-healing nanofiber-based composites: Static test and subcritical crack propagation, ACS Appl. Mater. Interfaces 8 (2016) 18462-18470.
[26] A.L. Yarin, B. Pourdeyhimi, S. Ramakrishna, Fundamentals and applications of micro- and nanofibers, Cambridge University Press, Cambridge, 2014.
[27] S. Jiang, G. Duan, U. Kuhn, M. Mörl, V. Altstädt, A.L. Yarin, A. Greine, Spongy gels by a top-down approach from polymer fibrous sponges, Angewante Chemie 56 (2017) 3285-3288.
[28] M.W. Lee, S.S. Yoon, A.L. Yarin, Release of self-healing agents in a material: What happens next?, ACS Appl. Mater. Interfaces 9 (2017) 17449−17455.
[29] K. Molnar, E. Kostakova, L. Meszaros, The effect of needleless electrospun nanofibrous interleaves on mechanical properties of carbon fabrics/epoxy laminates, Express Polymer Letters 8 (2014) 62-72.
[30] Y. Fang, C.-F. Wang, Z.-H. Zhang, H. Shao, S. Chen, Robust self-healing hydrogels assisted by cross-linked nanofiber networks, Scientific Reports 3 (2013) 2811.
[31] K.S. Toohey, N.R. Sottos, J.A. Lewis, J.S. Moore, S.R. White, Self-healing materials with microvascular networks, Nat. Mater. 6 (2007) 581-585.

Formatted: Not Highlight